



Preparation of MoO₂ sub-micro scale sheets and their optical properties

Xinli Liu, Yuehui He*, Shiliang Wang, Quan Zhang

State Key Laboratory of Powder Metallurgy, Central South University, Changsha, 410083; PR China

ARTICLE INFO

Article history:

Received 22 August 2010

Received in revised form 18 January 2011

Accepted 18 January 2011

Available online 22 January 2011

Keywords:

Molybdenum dioxide

Sub-micro sheets

Optical property

Growth mechanism

ABSTRACT

MoO₂ sub-micro sheets have been synthesized in a large scale on silicon substrate with MoO₃ and C powders as raw materials using a novel chemical vapour deposition method. The lengths and widths of MoO₂ sheets are in the range of several to dozens micrometers, and the thickness of MoO₂ sub-micro sheets is ~200 nm. Transmission electron microscopy and high-resolution electron microscopy show that the MoO₂ sheets are of single crystal with a monoclinic structure. The sheets exhibit fluorescent emissions at 304.4, 343.5 and 350.6 nm when the 220 nm light excitation is applied at room temperature, and the emissions result from some defects and the electron transition between valence band and conduction band. UV–vis spectrum shows the MoO₂ sub-micro sheets have absorption peaks between 200 and 300 nm and the emissions should be attributed to the defect states of MoO₂. Furthermore, the band-gap is estimated to be approximately 4.22 eV. The growth mechanism of the two-dimensional MoO₂ sub-micro scale sheets is also discussed.

© 2011 Elsevier B.V. All rights reserved.

1. Introduction

Transition metal oxides are large family of materials possessing various unique properties such as superconductivity, colossal magneto resistance, and piezoelectricity [1–3]. Among them, molybdenum dioxide possesses metallic electronic property, high melting point and is expected to be widely applied in the fields of catalysts, sensors, recording materials, and electrode materials [4–8]. Up till now, many methods have been employed to synthesize different morphologies of MoO₂. MoO₂ powder is traditionally prepared by reducing molybdenum trioxide with hydrogen at high temperature [8,9]. Yang et al. synthesized MoO₂ by reduction of MoO₃ with ethanol vapor. Manthiram et al. [10] and Liu et al. [4] have reported the preparation of MoO₂ powders by a reduction process in solution reaction routes. Liang et al. [11] synthesized different morphological MoO₂ nano-sized particles by a low temperature hydrothermal reaction. Porous and hollow spherical MoO₂ were synthesized by a hydrothermal reaction [7,12]. The one dimensional nanostructures of MoO₂ can be synthesized by carbon nanotubes templated growth [13], thermal evaporation [14–17] and some other methods [18]. For example: Zhou et al. [14] prepared large-scale MoO₂ nanowire arrays by thermal evaporation of Mo boat. Suemitsu et al. [19] synthesized MoO₂ hollow fiber on a Mo substrate heated with an acetylene–oxygen combustion

flame. However, there are few reports about the preparation of the two dimensional MoO₂ nanostructures. Yang et al. [20] obtained Tremella-like structured MoO₂ consisting of nanosheets via a Fe₂O₃-assisted hydrothermal reduction of MoO₃ in ethylenediamine aqueous solution.

Here, we report a novel method to synthesize MoO₂ sub-micro sheets by chemical vapor deposition using MoO₃ and C powders as reaction sources. Detailed morphology, structure and chemical composition analysis of the sheets are presented. Optical properties and growth mechanism are discussed.

2. Experimental details

The synthesis of MoO₂ sub-micro sheets was based on a horizontal tube furnace system. Starting materials used in this study were MoO₃ powders and graphite powders. The silicon substrate was first washed using hydrofluoric acid and then cleaned using alcohol in an ultrasonic cleaner to remove impurities from the substrate surface. Three alumina boats (named A, B, C), loaded respectively with 5 g MoO₃ powders, 1 g graphite powders, silicon substrate (20 mm × 10 mm × 1 mm) were pushed into the constant temperature zone of the furnace. Then the high-purity N₂ gas was introduced into the tube. Following that, the furnace was heated to 850 °C (heating rate: 6 °C/min) and maintained for 2 h, and the sample cooled to room temperature inside the furnace.

The morphology of the products was characterized by scanning electron microscopy (SEM, JSM-6360LV, 20 kV); the phase of the product was identified by X-ray diffraction (XRD, D/max 2550 VB with Cu Kα radiation); the structure of the MoO₂ sheets was

* Corresponding author at: Powder Metallurgy Research Institute, Central South University, Changsha, 410083, China. Tel.: +86 731 88836144; fax: +86 731 88710855.

E-mail address: yuehui@mail.csu.edu.cn (Y. He).

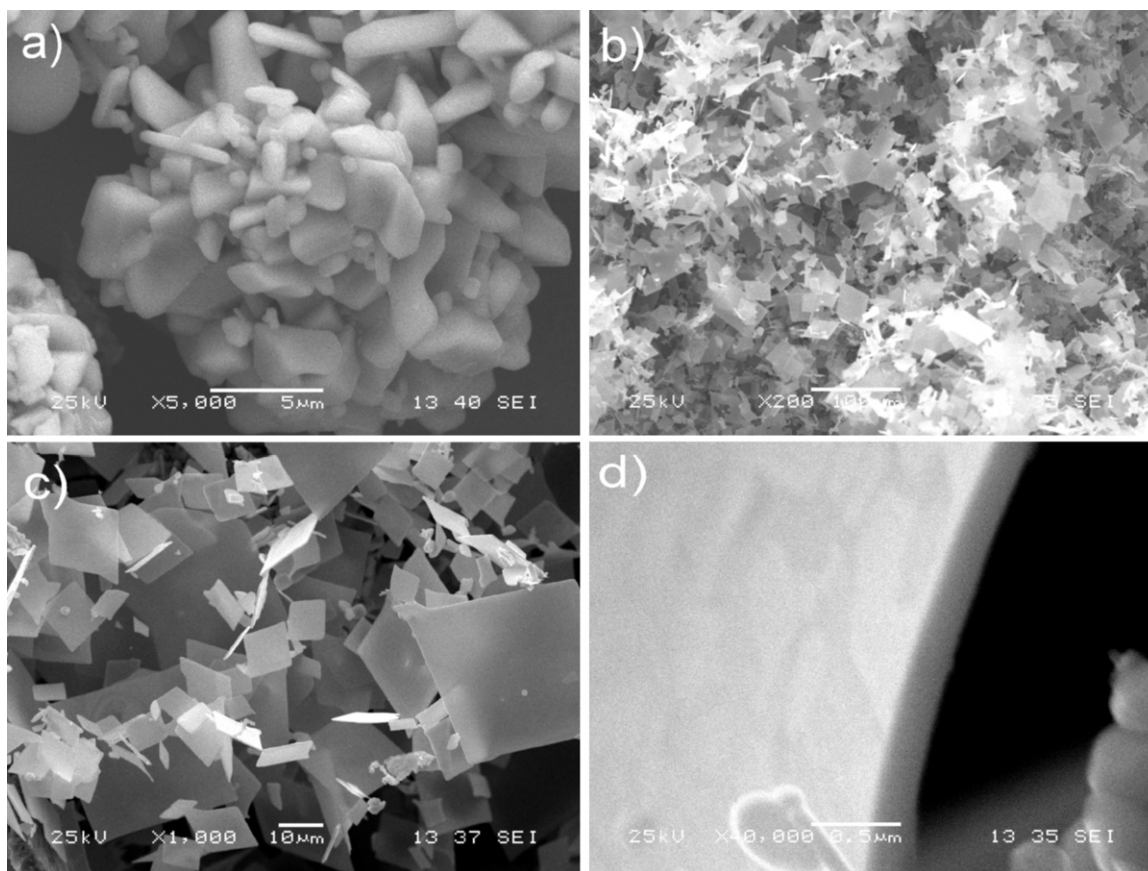


Fig. 1. (a) SEM image of the product from B boat, (b and c) different magnification SEM images of the sheet on the silicon substrates and (d) side view of the sheet.

analyzed by transmission electron microscopy (TEM, JEM-2100, 200 kV).

The optical properties of the as-synthesized MoO₂ sheets were measured on a fluorescence spectrophotometer (F-2500) under the excitation wavelength of 220 nm. The wavelength range is from 250 nm to 430 nm in our study and the scan speed is 300 nm/min. The slits width was adjusted to 5 nm. The UV-vis spectrum is obtained on a UV-vis spectrophotometer (TU-1800PC). The width of spectral band is 2 nm, and the scanning range is from 200 nm to 1100 nm. The sampling interval is 1 nm.

3. Results and discussion

Fig. 1(a–d) product taken from B boat and Si substrate. From **Fig. 1a**, it is observed that the morphology of the product on top of the graphite in B boat is powdered particle. **Fig. 1(b–d)** shows typical images of the sheets grown on the substrate, showing that the sheets are large-scale and well separate from each other, and also reveal that the MoO₂ sheets are square, uniform with a thickness of ~200 nm and lengths of ~30 μm. **Fig. 2(a and b)** presents the corresponding XRD pattern of the collected products from B boat and Si substrate, respectively. All diffraction peaks can be comprehensively indexed by the monoclinic MoO₂ structure with lattice parameters of $a = 0.5607$ nm, $b = 0.4859$ nm, $c = 0.5537$ nm, $\beta = 119.37^\circ$ (JCPDS: 32-0671), indicating that the products both from B boat and Si substrate are pure MoO₂ phase. However, there are also some remarkable differences between the two XRD patterns: the intensity of all the diffraction peaks of **Fig. 2a** is well consistent with the standard pattern, while in **Fig. 2b**, the diffraction peak of (–202) is the strongest, also revealing that the sheets have preferred orientation in [–101]. **Fig. 3a** shows the typical TEM image

of the as-synthesized MoO₂ sub-micro sheets. It is observed that the sheets have a uniform thickness and a shape of rectangle. Further structural characterizations were carried out by HRTEM and SAED (**Fig. 3b** and its inset). From the clear crystal lattices, we can see that the MoO₂ sheets are single crystal. Two sets of orthogonal parallel lattice fringes with spacing of 0.49 nm and 0.28 nm are corresponding to (020) and (101) atomic planes of monoclinic MoO₂, respectively. These crystal parameters are well consistent with that from the XRD data. It can also be regarded that the MoO₂ sheets may grow along two perpendicular directions: [010] and [101] to form 2D sheets.

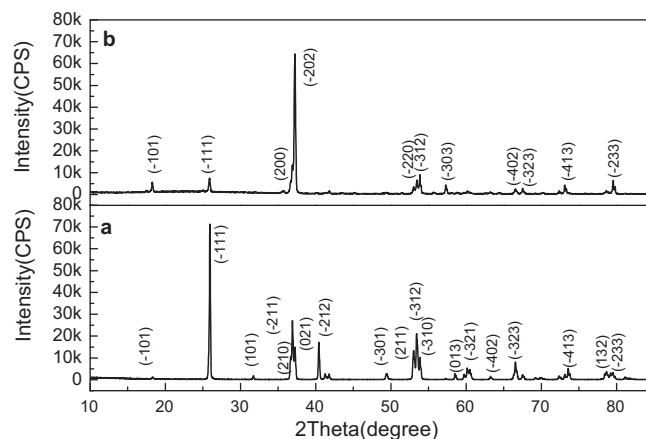


Fig. 2. (a) XRD patterns of the product, (a) from B boat, (b) from the silicon substrate of the C boat.

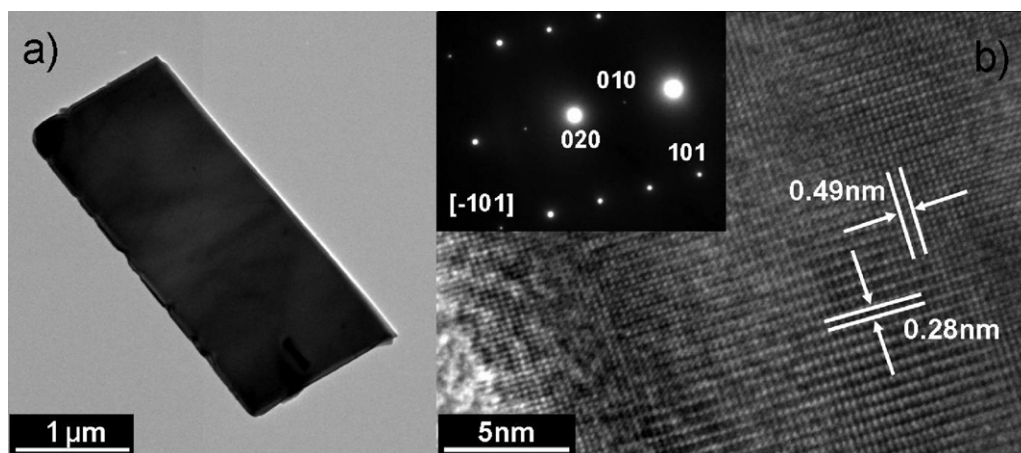
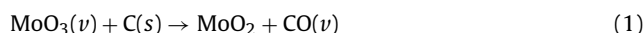


Fig. 3. (a) TEM image of a single MoO₂ sheet. (b) The HRTEM image, inset is the corresponding SAED pattern.

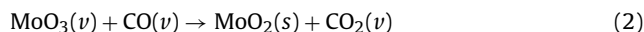
Based on the above-reported experimental results, we proposed that the formation of MoO₂ sub-micro sheets were governed by a chemical vapor deposition process which can be divided into two steps:

- (a) It is well known that MoO₃ begins to evaporate at temperature higher than 600 °C [21]. Therefore, firstly, as A boat is heated above 600 °C, MoO₃ begin to evaporate and this process would quickly take place after it is heated above its melting point (795 °C). Then when the furnace is holding at 850 °C, the vapor pressure of MoO₃ is up to 3.12 kPa, and plenty of gaseous MoO₃ carried by N₂ gas react with the graphite located in B boat:



According to the systematic calculation data of Gibbs free energy [18], the chemical reaction (1) can happen spontaneously to give rise to solid MoO₂ rather than gaseous MoO₂. So we observe some MoO₂ resultant with morphology of particle on the top of graphite in B boat.

- (b) Secondly, following the N₂, MoO₃ vapor continues to flow and react with the gaseous CO coming from reaction (1) and also generate solid MoO₂ on Si substrate. The reaction is



So MoO₂ solid phase produced by reaction (2) nucleated and grew into MoO₂ sub-micro sheets. Therefore, the vapor solid mechanism is likely responsible for the growth of MoO₂ sub-micro sheets in our experiment. It is well known that during crystal growth from the vapor, the super saturation degree of atom in the gaseous phase or vapor pressure of growth species has an important effect on the morphology of the grown crystal. With the increase of the gaseous source concentration, the grown crystal will in turn take the form of a one-dimension fiber, two-dimension plate, block and eventually a spherical particle [22]. Specifically, in our study, gaseous MoO₃ with bigger supersaturation on the top of boat B closed to boat A loaded with MoO₃ powder reacted with graphite and obtained MoO₂ particle, while on the top of boat C, the contention of gaseous MoO₃ decreased due to the large distance from boat A and the morphology of the product is sheet-like. So, the crystal nucleus grow into 2D sheets instead of 3D crystals or 1D whiskers maybe due to the moderate gas pressure of the reactant gas making the product nucleate in two dimensional and grow into sheets. So, the different morphologies of the resultants were mainly dependent on the concentration of the reaction gas.

According to the Wulff facets theorem [23], a crystal formed at equilibrium has to be bounded by facets, giving a minimum total surface energy. For monoclinic MoO₂, the close-packed plane is (0 1 0), and (1 0 1) can be the second closed-packed plane for monoclinic MoO₂. So (0 1 0) and (1 0 1) facets have larger surface area and lower surface energy, resulting in the preferred growth along [0 1 0] and [1 0 1] directions [24]. Hence, the resultant morphology of the crystals is sheet-like with minimum total surface energy.

The PL properties of the as-synthesized MoO₂ sheets were measured using a Xe lamp (150 W) as the excitation source at room temperature. Fig. 4 shows the emission spectrum. It is found that when the excitation wavelength is 220 nm, the emission peaks of the as-synthesized MoO₂ sheets consist of three UV emissions at 308 nm (4.1 eV), 346 nm (3.6 eV) and 397 nm (3.1 eV). At the same time, the emission of the single Si substrate is provided for comparison with MoO₂ sheets and no obvious emission peak is observed for a bare Si substrate. Thus, the possibility of emission peaks from the substrate is ruled out.

In order to investigate the luminescence mechanism of MoO₂ sheets, the optical gap of MoO₂ was measured by UV-vis spectrophotometer. The absorption spectrum of the MoO₂ was recorded in the wavelength range of 200–1100 nm at room temperature. The absorption coefficient α was calculated as a function [25] of the photon energy E from the absorption UV-vis spectrum.

$$(\alpha h\nu)^2 = B^2(h\nu - E_g) \quad (3)$$

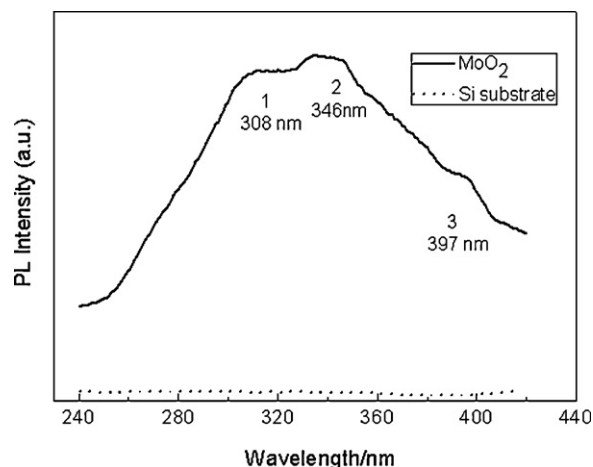


Fig. 4. PL spectrum of MoO₂ sub-micro sheets (solid —) and the Si substrate (dash ...) excited at 220 nm at room temperature.

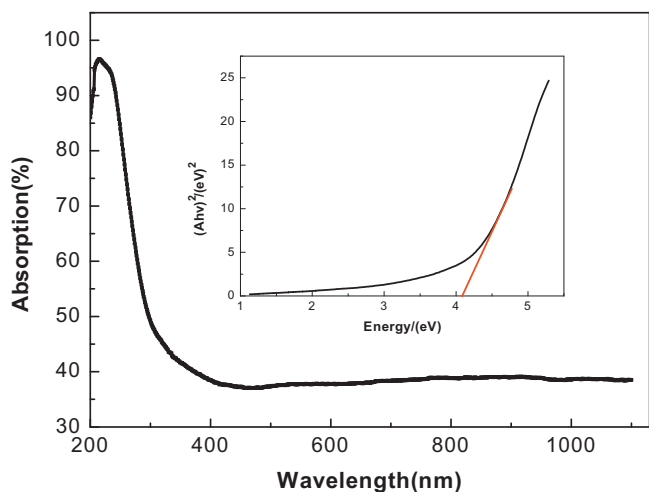


Fig. 5. UV-vis spectra of MoO₂ sub-micro sheet, the insert is the plots of $(Ah\nu)^2$ vs photon energy.

$h\nu$ is photon energy, α is absorption coefficient, B is a constant related to the material. E_g is optical band-gap. The absorptivity A is proportional to absorption coefficient, and according to the formula and the absorption spectra, a graph of $(Ah\nu)^2$ versus $h\nu$ was plotted as Fig. 5(insert). A linear rise near absorption edge indicates direct allowed transitions. Extrapolation of the straight-line portion to the zero absorption ($\alpha=0$) yield an E_g -value of 4.22 eV. The optical gap depends on the stoichiometry and structure of the Mo oxide investigated, a range of E_g -values have been reported in the literature for Mo oxide films [26–30] depending on the deposition method, deposition parameters, and film treatment [29]. Mohamed et al. [26] reported the optical band-gap of molybdenum oxide films was in the range of 2.64–2.69 eV and increased slightly with the increasing oxygen partial pressure. Lee et al. [30] obtained the E_g ranging from 3.0 to 3.5 eV according to the treatment methods of the MoO₃ film. It should also be noted that there are some uncertainties in the band-gap estimates using the Tauc method due to the nanograin structure [30]. While this value is very close to one of the UV emissions obtained at 304.4 nm (4.1 eV). So, this emission is likely to be attributed to the direct transition of electron between band and band, and the other two emissions may due to some defect states such as oxygen vacancies or the localized states in the band gap due to impurities, which are very common among metal oxides, such as ZnO [31] and WO_x [32,33]. Also, it is difficult to avoid the generation of other Mo oxides during the reaction process, so the emissions may also result from the few other oxides. The literatures about luminous performance of the Mo oxides are insufficient and this will be discussed further.

4. Conclusions

In summary, large scale MoO₂ sub-micro sheets with monoclinic structure have been prepared by a novel chemical vapor deposition using MoO₃ and C powders as raw materials. The products grow into 2D sheets maybe due to the moderate pressure of the reaction gas. The as-synthesized MoO₂ sub-micro sheets exhibit UV emis-

sions at 304.4 nm, 343.5 nm and 350.6 nm and UV-vis spectrum shows they have absorption peaks between 200 and 300 nm and the band-gap of the MoO₂ sub-micro sheet is 4.22 eV. The fluorescent emissions resulted from some defects and the electron transition between valence band and conduction band.

Acknowledgement

This project was supported by National Nature Science Foundation of China (no.50825102, 50804057, 51074188, 51071178, 50721003, and 50823006).

References

- [1] Y.Q. Zhu, W.B. Hu, W.K. Hsu, M. Terrones, N. Grobert, J.P. Hare, H.W. Kroto, D.R.M. Walton, H. Terrones, Chem. Phys. Lett. 309 (1999) 327–334.
- [2] W. Cheng, E. Baudrin, B. Dunn, J.L. Zink, J. Mater. Chem. 11 (2001) 92–97.
- [3] D.S. Lee, K.H. Nam, D.D. Lee, Thin Solid Films 375 (2000) 142–146.
- [4] Y. Liu, Y. Qian, M. Zhang, Z. Chen, C. Wang, Mater. Res. Bull. 31 (1996) 1029–1033.
- [5] A. Gulino, S.C. Parker, F.H. Jones, R.G. Egdell, J. Chem. Soc. Faraday Trans. 92 (1996) 2137–2141.
- [6] Y. Liu, Y. Qian, M. Zhang, Z. Chen, C. Wang, Mater. Sci. Eng. B 121 (2005) 152–155.
- [7] L.C. Yang, Q.S. Gao, Y. Tang, Y.P. Wu, R. Holze, J Power Sources 179 (2008) 357–360.
- [8] A. Katrib, J.W. Sobczak, M. Krawczyk, L. Zommer, A. Benadda, A. Jablonski, G. Maire, Surf. Interface Anal. 34 (2002) 225–229.
- [9] P. Wehrer, C. Bigey, L. Hilaire, Appl. Catal. A: Gen. 243 (2003) 109–119.
- [10] A. Manthiram, A. Dananjay, Y.T. Zhu, Chem. Mater. 6 (1994) 1601–1602.
- [11] Y.G. Liang, Z.H. Yi, S.J. Yang, L.Q. Zhou, J.T. Sun, Y.H. Zhou, Solid State Ionics 177 (2006) 501–505.
- [12] C.H. Guo, G.J. Zhang, Z.R. Shen, P.C. Sun, Z.Y. Yuan, Q.H. Jin, B.H. Li, D.T. Ding, T.H. Chen, Chin. J. Chem. Phys. 19 (2006) 543–548.
- [13] B.C. Satishkumar, A. Govindaraj, M. Nath, C.N.R. Rao, J. Mater. Chem. 10 (2000) 2115–2119.
- [14] J. Zhou, N.S. Xu, S.Z. Deng, J. Chen, J.C. She, Z. I. Wang, Adv. Mater. 15 (2003) 1835–1840.
- [15] J.Y. Zhang, Y.G. Liu, S.L. Shi, Y.G. Wang, T.H. Wang, Chem. Phys. B 17 (2008) 4333–4336.
- [16] J.G. Liu, Z.J. Zhang, C.Y. Pan, Y. Zhao, X. Su, Y. Zhou, D.P. Yu, Mater. Lett. 58 (2004) 3812–3815.
- [17] W. Merchan-Merchan, A.V. Saveliev, L.A. Kennedy, Chem. Phys. Lett. 422 (2006) 72–77.
- [18] F. Wang, B.Q. Lu, Phys. B 404 (2009) 1901–1904.
- [19] M. Suemitsu, T. Abe, H. Na, H. Yamane, Jpn. J. Appl. Phys. 44 (2005) 449–450.
- [20] L.C. Yang, Q.S. Gao, Y.H. Zhang, Y. Tang, Y.P. Wu, Electrochem. Commun. 10 (2008) 118–122.
- [21] O. Kubaschewski, C.B. Alcock, Metallurgical Thermochemistry, 5th ed., Pergamon, Oxford, 1979.
- [22] Y.J. Chen, J.B. Li, Y.S. Han, X.Z. Yang, J.H. Dai, J. Cryst. Growth 245 (2002) 163–170.
- [23] J.A. Venables, Introduction to Surface and Thin Film Process, Cambridge University Press, Cambridge, 2000.
- [24] G. Gu, B. Zheng, W.Q. Han, S. Roth, J. Liu, Nano Lett. 2 (2002) 849–851.
- [25] J. Tauc, F. Abeles (Eds.), The Optical Properties of Solids, North-Holland, Amsterdam, 1972.
- [26] S.H. Mohamed, O. Kappertz, J.M. Ngaruiya, T.P. Leervad Pedersen, R. Drese, M. Wuttig, Thin Solid Films 429 (2003) 135–143.
- [27] G.E. Buono-Core, G. Cabello, A.H. Klahn, A. Lucero, M.V. Nuñez, B. Torrejón, C. Castillo, Polyhedron 29 (2010) 1551–1554.
- [28] S.S. Sunu, E. Prabhu, V. Jayaraman, K.I. Gnanasekar, T.K. Seshagiri, T. Gnanasekaram, Sens. Actuators B 101 (2004) 161–174.
- [29] M.A.B. Moraes, B.C. Trasferetti, F.P. Rouxinol, R. Landers, S.F. Durrant, J. Scarmínio, A. Urbano, Chem. Mater. 16 (2004) 513–520.
- [30] Y.J. Lee, W.T. Nichols, D.G. Kim, Y.D. Kim, J. Phys. D: Appl. Phys. 42 (2009) 115419.
- [31] M. Feng, A.L. Pan, H.R. Zhang, Z.A. Li, F. Liu, H.W. Liu, D.X. Shi, B.S. Zou, H.J. Gao, Appl. Phys. Lett. 86 (2005) 141901.
- [32] M.J. Zheng, L.D. Zhang, G.H. Li, W.Z. Shen, Chem. Phys. Lett. 363 (2002) 123–128.
- [33] K. Lee, W.S. Seo, J.T. Park, J. Am. Chem. Soc. 125 (2003) 3408–3409.